

Experimental study of single- and double-electron-capture by Ne ions from He gas

A.T. Hasan^a

American University of Sharjah, Department of Physics, P.O. Box 26666, Sharjah, United Arab Emirates

Received 5 November 2004 / Received in final form 13 February 2005

Published online 24 May 2005 – © EDP Sciences, Società Italiana di Fisica, Springer-Verlag 2005

Abstract. In the present work, the total cross-sections for single- and double-electron-capture by low-energy highly-charged Ne^{q+} ($q = 2-6$) recoil ions from He atomic gas have been measured in the energy range 600–1000 eV/ q . These measurements are compared with other available experimental results. The charge state dependence of the single-electron-capture cross-sections for Ne^{q+} ($q = 2-6$) recoil ions incident on He at energy of 1000 eV/ q is compared with the theoretical predictions of the absorbing sphere model and the classical model.

PACS. 34. Atomic and molecular collision processes and interactions

1 Introduction

In recent years, we have been witnessing intensive experimental and theoretical research of electron transfer processes in atomic and molecular collisions. The reasons for this active research range from its fundamental importance in understanding the complex ion-atom reactions [1–18], testing the theoretical models [6–10] to their recognized role in high-temperature plasma applications [19, 20], astrophysics, atmospheric science [21] and atomic physics [22].

In the low energy range, total cross-section measurements are few and known to be affected by the ionic core [23] due to the strong repulsive Coulomb potential between the product ions. At these energies, for the lowest-charge states, the capture is favored only between ground states. For highly charged ions, capture is usually favored to several excited states of the final states of the product ions. Understanding the electron dynamics in low-energy collisions a detailed molecular description is needed, in which the crossing between molecular states and coupling of these states with the continuum play a fundamental role [24].

The main objectives of this paper are to provide a reliable measurement for the absolute total electron-capture cross-sections for the Ne^{q+} –He system in the low energy range 600–1000 eV/ q and to study the dependence of the single- and double-electron-capture cross-sections of Ne^{q+} on the physical parameters E^1 (the recoil ion energy) and the charge state q of the ion. We show our results and compare them later with the theoretical predictions. The availability of detailed experimental data allows stringent test to the existing predictions of theoretical models.

^a e-mail: ahasan@aus.ac.ae or ahasan@ausharjah.edu

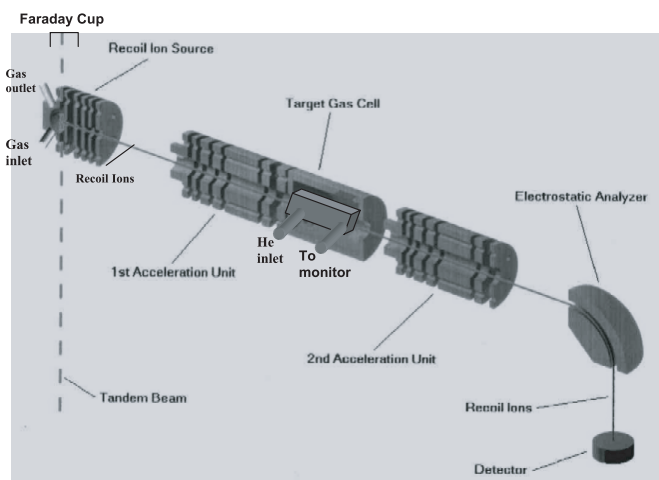


Fig. 1. Schematic diagram shows the experimental apparatus.

2 Experiment

2.1 Experimental set-up

Measurements of the atomic ion yield were made using the apparatus shown in Figure 1. It consists of recoil ion source (RIS), first acceleration unit, gas-target cell, second acceleration unit, electrostatic analyzer and detector. This apparatus [11–14, 25] was mounted inside a collision chamber with base pressure about 6×10^{-7} Torr. A pulsed and bunched 19-MeV F^{+4} beam from the tandem Van de Graaff accelerator at the Kansas State University was passed through the RIS containing Ne gas at 1 mTorr. Charged Ne recoil ions generated by the collisions in the RIS were extracted and accelerated by an applied electric

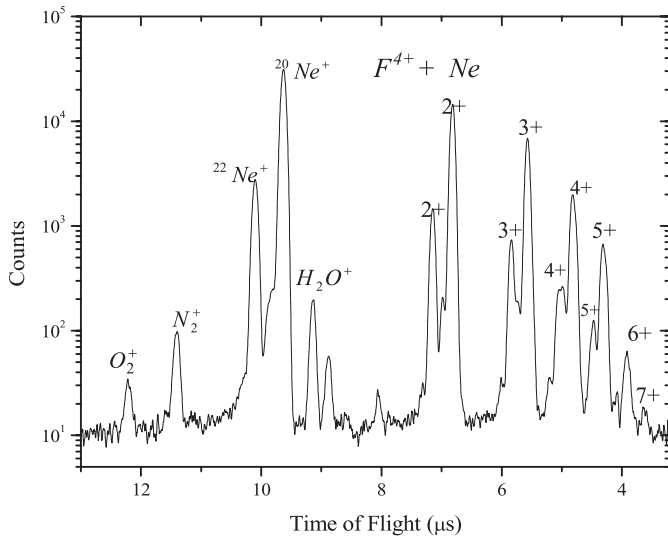


Fig. 2. Time-of-flight spectrum for Ne^{q+} recoil ions of 700 eV/ q energy.

field which is transverse to the beam direction. These ions were then directed through the first acceleration unit of 5.8 cm in length toward a differentially pumped gas-target cell containing He gas at a pressure of 0.8 mTorr. This gas-target cell pressure was measured by an MKS type 90 capacitance manometer and controlled by servoassisted gas-handling system which regulated a Granville-Phillips variable leak. A 5.8-cm long cell was used with entrance and exit apertures of 1 and 2.5 mm in diameter, respectively. It is field-free to avoid an undesired deflection of slow, highly charged ions. After leaving the gas-target cell, the emergent ions were traveled through the second acceleration unit, which is identical to the first acceleration unit, to a position sensitive channel-plate detector via a 90° hemispheric electrostatic analyzer with inner and outer radii of 3.25 and 3.75 cm, respectively.

The time-of-flight (TOF) of an ion from its production in the RIS to its detection at the detector provides the initial charge state q of the recoil ion since TOF of an ion is proportional $\sqrt{m/q}$, where m is the mass of the ion. Figure 2 shows a TOF spectrum for Ne^{q+} recoil ions produced by a 19-MeV F^{4+} beam. Representative charge states are identified in the figure. The peaks labeled N_2^+ , O_2^+ and H_2O^+ arise from the residual vacuum are also shown.

The use of the electrostatic analyzer in conjunction with the TOF technique allows one to identify the various events associated with the charged ions. The recoil ions pass through the secondary gas-target cell with a counting rate of approximately 1 kHz where charge-changing collision of the form



may take place. The recoil ions then are analyzed with the hemispherical electrostatic analyzer according to:

$$V = K \frac{q}{q-m} V_0,$$

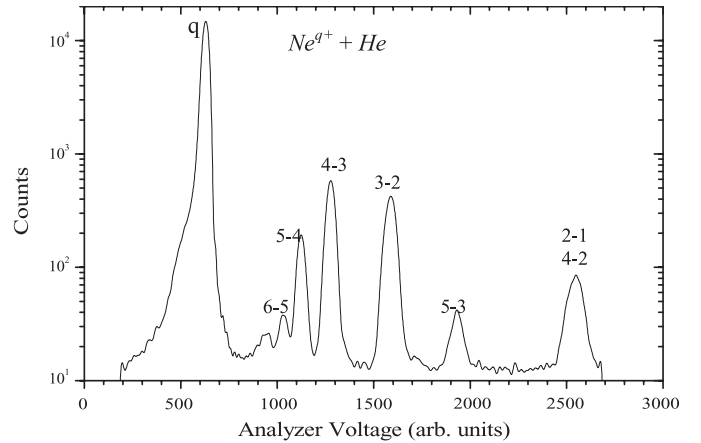


Fig. 3. Voltage sweep spectrum for 700 eV/ q Ne^{q+} recoil ions on He. The direct events peak is labeled q . The numbers on the electron capture peaks denote the initial recoil-ion charge state q , and the detected final charge state $q - m$, respectively.

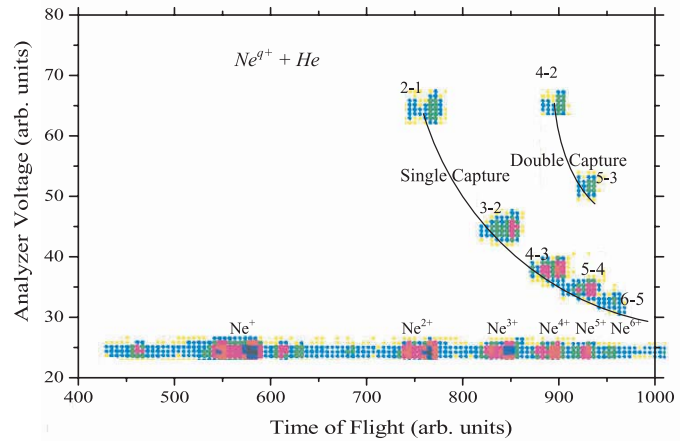


Fig. 4. Two-dimensional coincidence spectrum obtained for 700 eV/ q $\text{Ne}^{q+} + \text{He}$. The initial recoil-ions and single- and double-electron-capture loci are shown. A colour version of the figure is available in electronic form at <http://www.eurphysj.org>.

where V is the analyzer voltage, K is the analyzer constant, m is the number of the target electrons captured and qV_0 is the initial energy of the recoil ions. The voltage V from a programmable power supply was swept by a triangle wave generator to cover the energy range of ~ 20 eV to 550 eV. The lower limit of the energy corresponds to the condition that all the recoil ions that retain their initial charge states ($q = q - m$) are detected, for a fixed V_0 , at the same analyzer voltage. Electron capture events correspond to different values of the ratio $q/(q - m)$ as seen in the analyzer voltage spectrum are shown in Figure 3. Hence by creating a two dimensional array of V versus TOF, one builds a map of ion events which represents the electron-capture process. Typical two-dimensional spectrum of V versus TOF is shown in Figure 4. Initial recoil-ion charge state and the electron capture loci are shown in the figure.

Table 1. Single-electron-capture cross-sections $\sigma_{q->q-1}$ (10^{-15}cm^2) for $\text{Ne}^{q+} + \text{He}$ system.

$E(\text{eV}/q)$	$\sigma_{2,1}$	$\sigma_{3,2}$	$\sigma_{4,3}$	$\sigma_{5,4}$	$\sigma_{6,5}$
600	0.13 ± 0.019	1.02 ± 0.15	2.49 ± 0.40	2.9 ± 0.44	5.48 ± 0.82
700	0.15 ± 0.022	0.92 ± 0.14	3.23 ± 0.48	3.65 ± 0.55	6.02 ± 0.90
800	0.19 ± 0.028	1.18 ± 0.18	2.78 ± 0.42	3.35 ± 0.50	5.88 ± 0.88
900	0.20 ± 0.03	1.85 ± 0.28	3.49 ± 0.52	4.12 ± 0.62	6.02 ± 0.90
1000	0.22 ± 0.033	2.56 ± 0.38	3.56 ± 0.53	4.48 ± 0.67	6.44 ± 0.97

2.2 Electron-capture cross-sections

Under the thin target conditions (low gas-target pressure) used in this experiment which ensures single-collision conditions the absolute total cross-sections σ were deduced from:

$$\sigma = \frac{N_c}{N_t n \epsilon l}$$

where N_c is the measured number of the electron capture events of charge state $(q-m)$, N_t is the measured number of incident ions of the charge state q , n is the number of gas particles per cm^3 in the collision target-cell and is related the measured pressure p in Pa according to $n = 2.45 \times 10^{14} p$ (at 22°C), ϵ is the detection efficiency of detector and l is the geometric length of the target cell. For the efficiency of the channel-plate detector (32.4%), we used the product of the active area ratio of the first channel-plate from the manufacturer's manual, which is 60%, and the transmission of the grids at the entrance of the detector, which is 54% [25,26].

2.3 Error estimate

The error in the cross-sections originated mainly from the data fluctuations, counting statistics, gas pressure stability and the correction to the length of the gas-target cell. A correction for the cell length was made by adding the radii of the cell apertures to the measured length [27]. The counts from background gas were measured without the Ne^{q+} recoil ions and found to be less than 5% of the total counts. These counts were subtracted from the data.

The total absolute uncertainty of cross-section was obtained as the quadrature sum of the counting statistics and the systematic uncertainties of all measured quantities. The total absolute uncertainty is estimated to be about 15%. The data, including the total uncertainty, are presented in Tables 1 and 2 and shown in Figures 5–11.

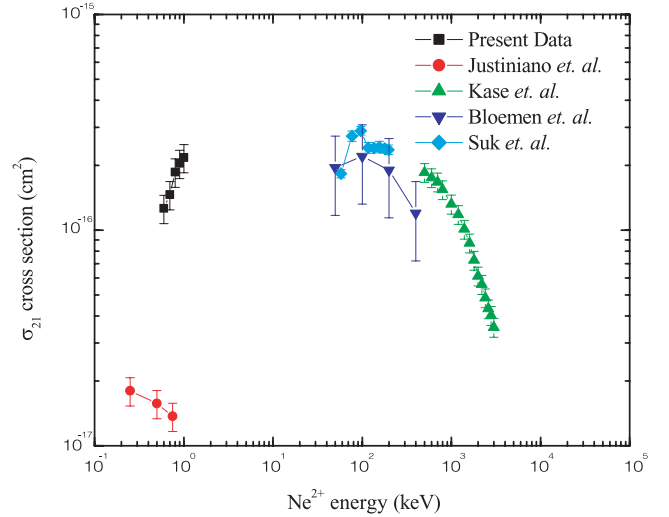
3 Results and discussion

3.1 Single-electron-capture cross-sections

The absolute total single-electron-capture cross-sections for $\text{Ne}^{q+} + \text{He}$ in the energy 600–1000 eV/ q for charge states $q = 2-6$ are measured and compared with other available data [1–5].

Table 2. Double-electron-capture cross-sections $\sigma_{q->q-2}$ (10^{-16}cm^2) for $\text{Ne}^{q+} + \text{He}$.

$E(\text{eV}/q)$	σ_{4-2}	σ_{5-3}
600	1.87 ± 0.28	2.66 ± 0.40
700	2.11 ± 0.28	3.10 ± 0.47
800	2.54 ± 0.38	3.66 ± 0.55
900	3.50 ± 0.53	4.49 ± 0.67
1000	4.77 ± 0.72	5.36 ± 0.81

**Fig. 5.** Single-electron capture cross-section for $\text{Ne}^{2+} + \text{He}$ collision.

3.1.1 $\text{Ne}^{2+} + \text{He}$ collisions

As shown in Figure 5, the general shape of the cross-section reported in this paper for this collision shows a monotonically increasing behavior as a function of incident energy. The present low-energy data and previous high-energy data [2–5] display a bell-shaped cross-section centered at approximately 10 keV (see Fig. 5). This behavior is typical of single-electron-capture cross-sections between singly-charged ions and neutral atoms for which capture is usually favored only between atomic ground states. A lack of experimental data that cover a wide energy range 1–40 keV and a disagreement between the present data and those of Justiniano et al. [1] are depicted in Figure 5. There is evidently further work to be done to resolves these two problems.

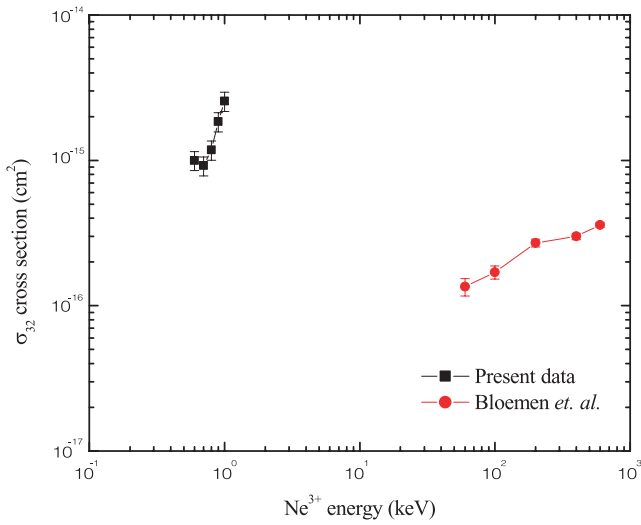


Fig. 6. Single-electron capture cross-section for $\text{Ne}^{3+} + \text{He}$ collision.

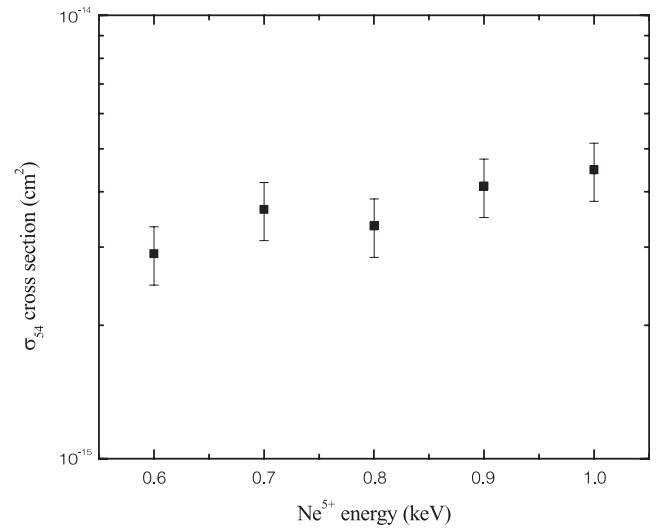


Fig. 8. Single-electron capture cross-section for $\text{Ne}^{5+} + \text{He}$ collision.

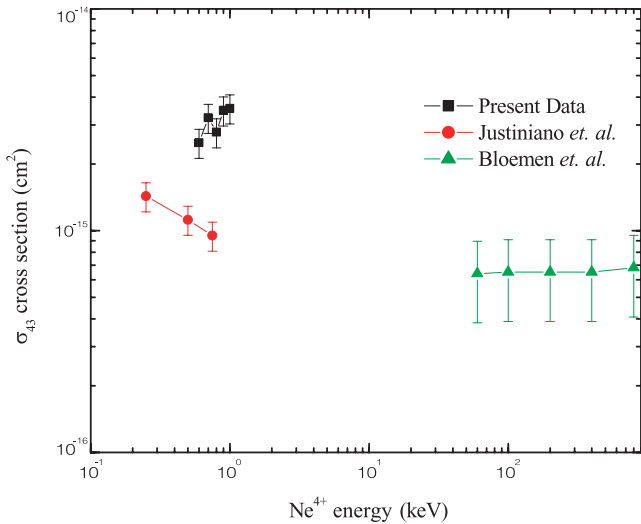


Fig. 7. Single-electron capture cross-section for $\text{Ne}^{4+} + \text{He}$ collision.

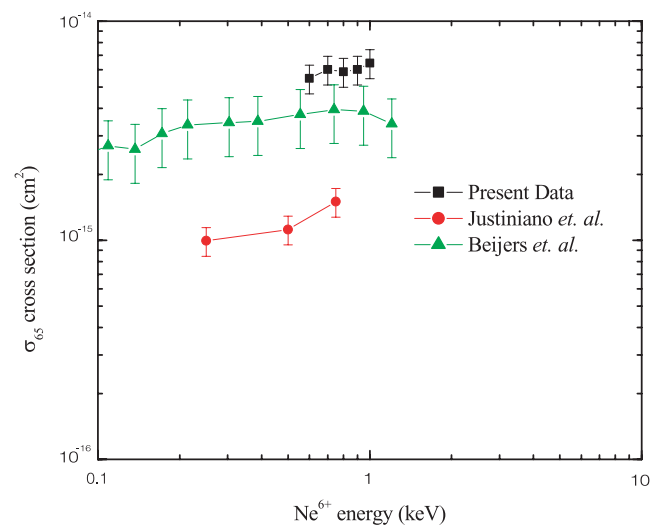


Fig. 9. Single-electron capture cross-section for $\text{Ne}^{6+} + \text{He}$ collision.

3.1.2 $\text{Ne}^{3+} + \text{He}$ collisions

The present low energy data and the high energy measurements of Bloemen et al. [2] are shown in Figure 6. The cross-sections in both measurements increase as the collision energy increases. From close inspection of Figure 6, the present data is in poor accord with the high energy data [2].

3.1.3 $\text{Ne}^{4+} + \text{He}$ collisions

The present measurements and other available data are shown in Figure 7. The present data display approximately similar cross-section magnitudes as the collision energy increases. The present results are in significant disagreement with the results of Justiniano. The high energy results of Bloemen almost identical cross-section magnitudes as the collision energy increases.

3.1.4 $\text{Ne}^{5+} + \text{He}$ collisions

The dependence of the present cross-sections on the collision energy is shown in Figure 8. These cross-sections show rather flat energy dependence. Lack of previous data in the literature hinders a comparison.

3.1.5 $\text{Ne}^{6+} + \text{He}$ collisions

Total cross-sections for single electron capture of Ne^{6+} in He gas is shown in Figure 9. The present data are compared with other available measurements [1,5]. The present data agree within the uncertainties of those data of Beijers et al. [5] and are inconsistent with those data of Justiniano's et al. [1]. Such disagreement could be ascribed to the different experimental techniques used. Considering the disagreement between these measurements, there is evidently further work to be done to resolve this problem.

The general shape of the cross-section for this reaction shows a rather flat behavior as a function of incident energy.

For $q > 3$ the measured cross-sections are all large and independent of energy in the range currently tested. The energy independent cross-sections are due to the availability of many exoergic channels and one needs to consider mainly the final states of the final ions which yield to reasonable crossing radii.

3.2 Dependence of the sections on the initial charge state

The dependence of single-electron-capture cross-sections on the initial charge state of $1000 \text{ eV}/q$ Ne^{q+} ions are shown in Figure 10. The predictions of the absorbing sphere model [Appendix A] and the classical model [Appendix B] are also shown in this figure for comparison. The cross-sections increase with the charge state. The present measurements show a relatively small cross-section for $q = 2$. For a given energy/charge state the classical model predicts an oscillatory dependence of the cross-sections on the charge state q . Such oscillations in the cross-sections have not been seen in the Ne^{q+} -He system and the present measurements are in disagreement with the predictions of the classical model. The absorbing sphere model does not predict such oscillatory dependence of cross-sections on the charge state q but rather a smooth increase of cross-section with q . The present data follow the predictions of the absorbing sphere model except for $q = 2$. The measured cross-section for single-electron-capture by Ne^{2+} from He is smaller by an order of magnitude than that of the predictions of the absorbing sphere model.

3.3 Double-electron-capture cross-sections

The general features of the double-electron-capture cross-sections of Ne^{q+} ($q = 4, 5$) incident on He from the present data and the results of Justiniano plotted as a function of the projectile collision energy are illustrated in Figure 11. Due to the complexity of the system under study and the lack of the predictions of theoretical models to describe such system these features will be presented qualitatively. The present data show slow increase in the cross-sections with increasing collision energy. These double-electron-capture cross-sections for $\text{Ne}^{4,5+}$ are by far smaller than the corresponding single-electron-capture cross-sections. The present data are in fair accord with Justiniano's results.

4 Conclusion

The main purpose of this paper is to present the experimental data on absolute total single- and double-capture cross-sections of Ne^{q+} recoil ions by He noble gas at low energy. The charge state and the energy dependence of these measured cross-sections are explored. The

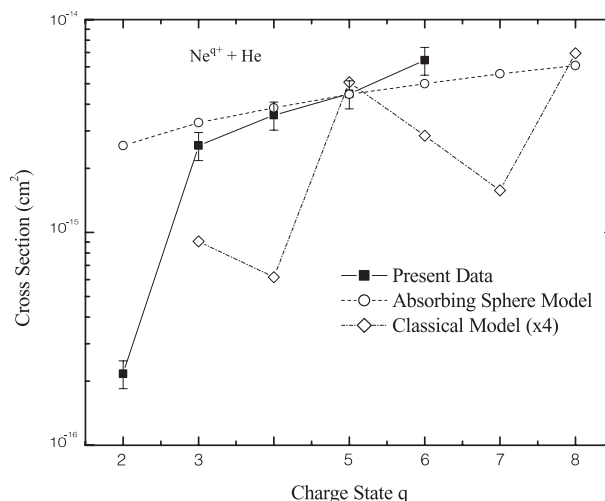


Fig. 10. shows the dependence of single-electron-capture cross-sections on the initial charge state of the recoil ions for the collision of Ne^{q+} at energy of $1000 \text{ eV}/q$ with He. Lines are drawn to guide the eye.

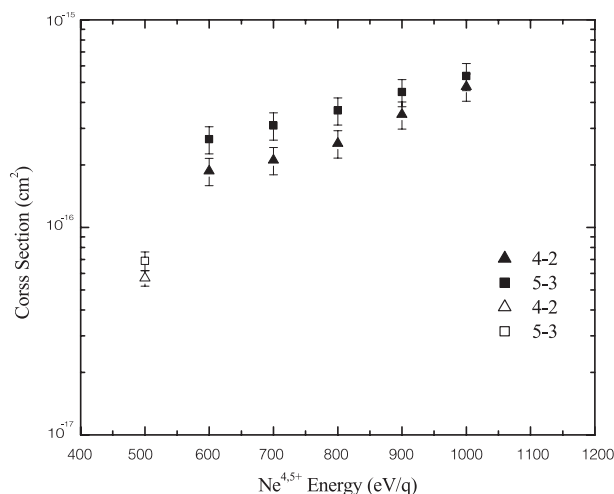


Fig. 11. Double-electron-capture cross-section for $\text{Ne}^{4,5+}$ + He. The present results are shown by filled symbols and Justiniano's data are shown by open symbols.

charge state dependence of the single-electron-capture cross-sections is found to be in quite consistent with the predictions of the absorbing sphere model except for $q = 2$ and in poor accord with the classical model.

As was mentioned in the introduction, the measurements of low-energy electron-capture cross-sections can be used in testing theoretical models. Accurate theoretical calculations are still needed to resolve the discrepancies reported in this paper between the present measurements and other available experimental results [1–5].

The author gratefully acknowledges with thanks the experimental support, discussion and useful suggestions of Dr. T.J. Gray. I also thank the accelerator crew of the J.R. McDonald laboratory at Kansas State University for providing a high quality beam during the course of the experiment.

Appendix A: Absorbing sphere model

Olson and Salop [6] developed a reduced coupling matrix-element formula for application to the charge-changing collisions of the form

$$X^{q+} + T \rightarrow X^{(q-1)+} + T^+.$$

The reduced coupling matrix elements with the absorbing-sphere model based on the Landau-Zener theory have been used to calculate the electron-capture cross-sections for fully-stripped ions colliding with neutral targets. The authors assumed unit probability for reaction inside some critical crossing radius, R_c in atomic units

$$R_c^2 e^{-2.648\alpha R_c/q^{1/2}} = 2.864 \times 10^{-4} q(q-1)v_0/f,$$

where $\alpha = [I_t(\text{eV})/13.6]^{1/2}$, I_t is the ionization potential of target atom, f is the Franck-Gordon factor for the specific transition between the vibrational levels and v_0 is the incident velocity measured in atomic units. The charge-exchange cross-section can then be obtained from

$$\sigma_{\text{OSAM}} = \pi R_c^2.$$

The basic assumption of this model that there are a large number of curve crossing at the intermolecular separation around R_c . If this condition does not hold, the authors suggest that the R_c calculated above should be used together with the energy defects obtained from the energy level tables.

Appendix B: Classical model

In this model the capture [7,8] of electron by Ne^{q+} is dominated by an energy gain which can be correlated to the principal quantum number n_c of the projectile. This number into which capture occurs is given by

$$n_c \leq \left[2|I_t| \left(1 + \frac{Z_{\text{eff}q}^{-1}}{2Z_{\text{eff}q}^{1/2} + 1} \right) \right]^{1/2},$$

where I_t is the ionization potential of target, the charge state of the recoil ion and $Z_{\text{eff}q}$ is the effective charge of the recoil ion. Only electron capture to np state was considered in calculating $Z_{\text{eff}q}$. The capture is assumed to occur at a critical crossing radius, R_c in atomic units

$$R_c = \frac{Z_{\text{eff}q} - 1}{\frac{Z_{\text{eff}q}^2}{2n_c^2} - I_t}.$$

Assuming the probability for electron capture to be 1/2, the cross-section was calculated from

$$\sigma_{\text{CLM}} = \frac{1}{2} \pi R_c^2.$$

This classical model predicts strong oscillatory dependence of the cross-sections on the charge states of the incident ions. However, it neglects any dependence on the velocity of the recoil ion.

References

1. E. Justiniano, C.L. Cocke, T.J. Gray, R. Dubois, C. Can, W. Waggoner, Phys. Rev. A **29**, 1088 (1984)
2. E.W.P. Bloemen, D. Dijkkamp, F.J. de Heer, J. Phys. B **15**, 1391 (1982)
3. M. Kase, A. Kikuchi, A. Yagishita, Y. Nakai, J. Phys. B **17**, 671 (1984)
4. H.C. Suk, A. Guilbaud, B. Hird, J. Phys. B **11**, 1463 (1978)
5. J.P.M. Beijers, R. Hoekstra, R. Morgenstern, F.J. de Heer, J. Phys. B **25**, 4851 (1992)
6. R.E. Olson, A. Salop, Phys. Rev. A **14**, 579 (1976)
7. R. Mann, F. Folkmann, H.F. Beyer, J. Phys. B **14**, 1161 (1981); R. Mann, F. Folkmann, H.F. Beyer, Phys. Rev. Lett. **46**, 646 (1981)
8. H. Ryufuku, K. Sasaki, T. Watanabe, Phys. Rev. A **21**, 745 (1980)
9. R. E. Olson, J. Foil, J. Phys. B **36**, L365 (2003)
10. C. Illescas, A. Riera, J. Phys. B **31**, 2777 (1998)
11. A.T. Hasan, J. Electron Spectrosc. Rel. Phen. **135**, 159 (2004)
12. A.T. Hasan, T.J. Gray, Int. J. Mol. Sci. **4**, 284 (2003)
13. A.T. Hasan, T.J. Gray, Nucl. Instr. Meths. B **198**, 1 (2002)
14. A.T. Hasan, T.J. Gray, Int. J. Mod. Phys. E **11**, 567 (2002)
15. C. McGrath, M.B. Shah, P.C.E. McCartney, J.W. McConkey, Phys. Rev. A **64**, 062712 (2001)
16. D.M. Kearns, R.W. McCullough, H.B. Gilbody, J. Phys. B **35**, 4335 (2002)
17. P. Sobocinski, J. Rangama, G. Laurent, L. Adoui, A. Cassimi, J.-Y. Chesnel, A. Dobois, D. Hennecart, X. Husson, F. Fremont, J. Phys. B **35**, 1353 (2002)
18. P.G. Reyes, F. Castillo, H. Martinez, J. Phys. B **34**, 1485 (2001)
19. R.K. Janev, Summery Report of Second Research Coordination meeting on *Atomic and Molecular Data for Plasma Edge Studies*, International Energy Report (Vienna, 1993), p. 276
20. C.F. Maggi, I.D. Horton, H.P. Summer, Plasma Phys. Control Fusion **42**, 669 (2000)
21. D. Pequignot, Astron. Astrophys. **81**, 3561 (1980)
22. S. Datz, G.W.F. Drake, T.F. Gallagher, H. Kleinpoppen, G. Zu, Putitz, Rev. Mod. Phys. **71**, S223 (1999)
23. R.A. Phaneuf, I. Alvarez, F.W. Meyer, D.H. Crandall, Phys. Rev. A **26**, 1892 (1982)
24. J. Delos, Rev. Mod. Phys. **53**, 287 (1981)
25. T.G. Gray, I. Ben-Itzhak, N.B. Malhi, V. Needham, K. Cranes, J.C. Legg, Nucl. Instr. Meth. B **40**, 1049 (1989)
26. B. Brehm, J. Grosse, T. Ruschinski, M. Zimmer, Meas. Sci. Technol. **6**, 953 (1995)
27. D.H. Crandall, M.L. Mallory, D.C. Kocher, Phys. Rev. A **15**, 61 (1977)